

Biocompatibility of silicon nitride produced via partial sintering & tape casting

Berivan Cecen^a, Gulsum Topates^{b,1}, Aylin Kara^{c,1}, Serdar Onat Akbulut^{b,d},
Hasan Havitcioglu^{a,e}, Leyla Didem Kozaci^{f,g,*}

^a Institute of Health Science, Department of Biomechanics, Dokuz Eylül University, 35340, Izmir, Turkey

^b Department of Metallurgical and Materials Engineering, Ankara Yildirim Beyazit University, 06010, Ankara, Turkey

^c Department of Bioengineering, Izmir Institute of Technology, 35430, Urla, Izmir, Turkey

^d Institute of Natural Sciences, Department of Bioengineering, Hacettepe University, 06800, Ankara, Turkey

^e Faculty of Medicine, Department of Orthopedics and Traumatology, Dokuz Eylül University, 35340, Izmir, Turkey

^f Institute of Health Science, Department of Translational Medicine, Ankara Yildirim Beyazit University, 06800, Ankara, Turkey

^g Turkey Faculty of Medicine, Department of Medical Biochemistry, Ankara Yildirim Beyazit University, 06800, Ankara, Turkey

ARTICLE INFO

Keywords:

Silicon nitride

Porosity

Tape casting

SaOS-2 human osteosarcoma cells

ABSTRACT

The biocompatibility of silicon nitride ceramics was proven by several studies however this study is apart from the literature in the manner of production routes that are tape casting and partial sintering. We report the tape casting route was chosen and a porous structure was obtained by partial sintering technique. Tape casting brought a smooth surface to the samples. Density and pore size distribution analysis showed that the scaffolds have low density because of the porous structure. XRD and SEM analyses were carried out to reveal the phase and microstructural characteristics of porous ceramic samples. Static contact angle measurement was done for the characterization of the wettability of the scaffolds. It revealed that the surface of the scaffolds was highly hydrophilic which is a desirable characteristic for the protein and cell adhesion. The mechanical characteristics of the scaffolds were analyzed by compression tests. Human osteosarcoma cells were used for *in vitro* studies. Cell-proliferation and cytotoxicity were analyzed by WST-1 and LDH, respectively. The osteoblastic behavior of the cells on the surface of the scaffolds was identified by alkaline phosphatase activity. BCA analysis was used for total protein content. The BCA and ALP results showed an increasing trend which is directly correlated with cell proliferation. Cells on the surface of the silicon nitride scaffolds were visualized by SEM and fluorescence microscopy where the images supported the *in vitro* analysis. Therefore, porous silicon nitride scaffolds fabricated via tape casting and partial sintering were biocompatible and they are possible candidates as bone substitute elements.

1. Introduction

Silicon nitride ceramics have been preferred in various industrial applications due to the perfect combination of their chemical, thermal, tribological and mechanical properties [1–3]. The possible usability of silicon nitride as a bone substitute or an implant was proven with various studies. Owing to the low mechanical properties of commercial ceramic bone grafts (e.g calcium phosphate-based ceramics) alternative ceramics have been investigated [4–6]. Since silicon nitride ceramic is one of the potential candidates for orthopedic implants, the studies mostly covered the production and characterization of dense silicon

nitride ceramics [2]. Several studies have focused on the fabrication of porous silicon nitride. Reaction bonded silicon nitride (RBSN), replica and pore former addition are examples of methods used for the production of porous silicon nitride. Porous silicon nitride that mimicked the cancellous structure of the human bone was produced via the replica technique. The pore characteristics and mechanical properties of air-sintered porous silicon nitride have the closest values to the trabecular bone and better cell viability and cell proliferation were observed compared to RBSN [7,8]. In another study, sintered RBSN (SRBSN) ceramics were studied. The proliferation of osteoblast-like cells was decreased when the RBSN technique was used compare to SRBSN.

* Corresponding author. Faculty of Medicine, Department of Medical Biochemistry, Ankara Yildirim Beyazit University, 06800, Ankara, Turkey.

E-mail address: dkozaci@gmail.com (L.D. Kozaci).

¹ These authors contributed equally.

Among these two types of silicon nitride ceramics, SRBSN favored the metabolism of the MG63 osteoblast cell [9–11]. *In vitro* characterization of the samples showed that mesenchymal stromal cells (MSC) proliferated and differentiated on the silicon nitride. Based on the *in vitro* cultures, the mesenchymal cells attach better to the edges than of the surfaces for the sample fabricated by pore former method [4,12,13]. Beside production techniques, porosity and surface properties (roughness and functions) are effective parameters on cell viability and proliferation capacity of silicon nitride ceramics. Tape casting offers highly qualified surface properties and samples are produced by this method do not require any surface treatments. In addition, tapes enable the samples with various dimensions by lamination of the casted ceramic tapes. Recent studies were showed that silicon nitride has a unique surface and that helps to osteoprogenitor cell growth and bony hydroxyapatite formation by human osteoblast cells. The surface energy of the silicon nitride-based on the broken bonds. When the density of broken bonds increases, there will be a decrement on the contact angle and increment on the surface energy. For silicon nitride, the small decrease in the contact angle has a direct factor on the precipitation of calcium phosphate within cell culture medium and which causes hydroxyapatite formation. HA maintains the hydrophilicity of the surface which promotes cell proliferation and differentiation [14,15]. Also, the heat treatments affect the surface properties which influence cell growth. Firing within the N₂ atmosphere at high temperatures improves the surface properties and has beneficial effects on cell growth, proliferation and attachment. In the N₂ annealed silicon nitride ceramics, many of the N- vacancies and positively charged N–N bonds are present on the surface. These bonds and sites reduce the negative surface charge which produced by amphoteric silicons at physiological pH. These unique surface characteristics make the silicon nitride antibacterial [16]. Related studies showed that a polished silicon nitride surface promotes cell yield, proliferation of osteoblast cells and greater osteocalcin production [3,17,18]. Among the shaping techniques of ceramics, tape casting enables the production of a surface, which is extremely smooth and flat and may eliminate the necessity of extra polishing step. Therefore, in current work, silicon nitride ceramic produced by tape casting technique was used and, biocompatibility and cell viability of silicon nitride were assessed. We believe that this work to have potential outlooks for various tissue engineering applications, such as 3D bone structure as possible candidates.

2. Materials and methods

2.1. Materials

Dulbecco's Modified Eagle Medium (DMEM, Sigma-Aldrich), fetal bovine serum (FBS-Lonza), penicillin-streptomycin-amphotericin B solution (Biological Industries) and L-glutamine (Sigma-Aldrich) were used for cell culture studies. Lactate dehydrogenase (LDH) kit (Thermo Fisher Scientific) and Cell Proliferation Reagent WST-1 (Roche Applied Science, Rotkreuz, Switzerland) were used to determine cell cytotoxicity and proliferation respectively. Bicinchoninic acid assay (BCA) kit (Thermo Fisher Scientific) was used to determine total protein content. Alkaline Phosphatase Activity Assay kit (ALP Assay, Enzyline PAL Optimise; Biomérieux, France) was used to determine ALP (alkaline phosphatase) activity. Paraformaldehyde (PFA, Merck) was used for cell fixation. Fluorescence staining reagents, DAPI (NucBlue), Alexa Flour 555 (Actin Red) were purchased from Thermo Fisher Scientific.

2.2. Scaffold preparation

α -silicon nitride (UBE SN E10, Japan) and CaO with 1.25 wt % (CaCO₃, Reidel-de Haen, Germany) were used as starting materials. Powders were mixed with ball mill at 180 rpm for 24 h in isopropyl alcohol. The rotary evaporation process was applied to dry powders. Tape casting was preferred for shaping the silicon nitride. Tape solution

was mixed with starting powders by using Dual Asymmetric Centrifugal Mixer (SpeedMixer™ (DAC150.1 FVZ)) for 20 min at 3000 rpm. Tape solution contains binders, anti-foaming & dispersing agents and alcohol. These agents provide homogeneously mixed and dispersed powder and aqueous solutions. Additionally, after casting process for preventing the breakages, plasticizer was used. The solid ratio of tape slurry was fixed to 40 wt %. The slurry was cast onto a silicone-coated polyester sheet and formed into tape by using a blade with a thickness of 400 μ m. Casted tapes were cut into 15 \times 15 mm² square shapes and 45 layers were laminated then they were pressed by using the uniaxial press (MSE Technologies) under 10 MPa pressure. Tapes were laminated before pressing. The final dimension of samples reduced to 5 \times 5x5 mm³ for *in vitro* studies. Reducing of the dimensions were done after sintering process. Tape casting is a favorable and well-known technique because the dimension can be tailored easily. The surfaces of the green samples were smooth lamination because of using the casting process. The surface quality did not change after heat-treatment. Before the sintering process, samples were subjected to a burn-out process. The heating rate was 0.5 °C/min up to 750 °C. Sintering was carried out under nitrogen atmosphere at 1700 °C for 3 h with a heating rate of 7 °C/h.

2.3. Physical characterization of specimens

Samples were defined using physical characteristics such as density, porosity and microstructure. Bulk densities and apparent porosities of the samples were determined by Archimedes' displacement principle according to ASTM C-20. Phase characterization was performed by X-ray diffraction (XRD) (Rigaku Miniflex 600) by using monochromatic Cu-K α radiation ($\lambda = 1.5406 \text{ \AA}$). The microstructure of the scaffolds was analyzed by using a scanning electron microscope (SEM) (Hitachi SU5000). The pore sizes and pore size distribution were analyzed by using mercury intrusion porosimetry (MIP) (Micromeritics, Autopore IV). Due to the non-wetting characteristic of mercury has been used in this technique. Under certain pressure, mercury penetrates pores and this pressure is inversely proportional to the size of the pores. Pore diameter-pressure relationship was determined by Washburn equation:

$$D = -4\gamma \cos\theta/P \quad (1)$$

where D: pore diameter; P: pressure [19].

2.4. Contact angle measurement

The wettability of the Si₃N₄ scaffolds was determined with the contact angle measuring system (Attension Theta Lite Optical Tensiometer). 1 \times 1 cm dimension of samples were prepared. Five independent measurements were performed by dropping 3 μ l size of ultrapure water onto the different positions of the scaffold surface. All data were analyzed using One Attension Software and determined as the mean values of measurements.

2.5. Mechanical test of scaffolds

Mechanical properties of Si₃N₄ scaffolds were evaluated with a compression test (5 kN AG-X; Shimadzu, Kyoto, Japan) according to ASTM-D 5024-95a standard. Compression was performed under axial direction with 1 mm/min crosshead speed up to failure. Elastic modulus and maximum stress were calculated based on the strain and stress data. Mechanical compression data was described as an average of five test specimens with standard error.

2.6. *In vitro* studies

2.6.1. Cell proliferation on scaffolds

SaOS-2 human osteosarcoma cells were cultured in DMEM supplemented with 10% FBS, 1% L-glutamine and 1% streptomycin-penicillin-

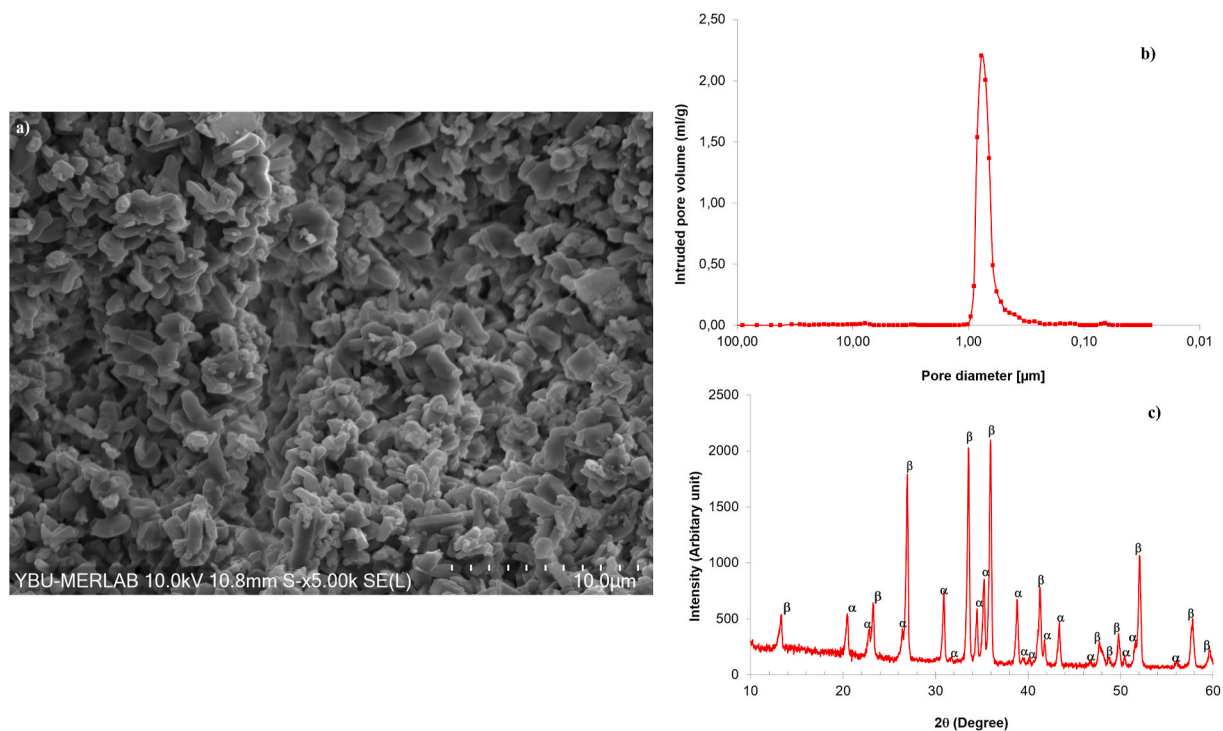


Fig. 1. a) SEM - SE images of silicon nitride ceramic b) Pore size distribution of the silicon nitride ceramic c). XRD pattern of silicon nitride sample (α : α -silicon nitride, β : β -silicon nitride). (For interpretation of the references to color in this figure legend, the reader is referred to the Web version of this article.)

amphotericin at 37 °C in a humidified 5% CO₂ atmosphere. Cells were sub-cultured for 7 days. Before cell seeding, silicon nitride scaffolds were sterilized at 90 °C with ethylene oxide. Cells (2×10^6 cell/mL) were seeded on scaffolds ($5 \times 5 \times 5$ mm³) and incubated at 37 °C, 5% CO₂ for 3, 7 and 10 days. WST-1 cell proliferation assay was used to detect the proliferation of cells. The absorbance was measured by a plate reader (Varioskan Flash, Thermo Fisher Scientific) at 440 nm wavelength.

2.6.2. Cytotoxicity assay

LDH (lactate dehydrogenase) activity was used as an indicator of cell membrane integrity. Cytotoxicity resulting from residual chemical compounds or processing methods was assessed using a kit commercially available by a plate reader at a reference wavelength of 450 nm.

2.6.3. Alkaline phosphatase activity

The alkaline phosphatase activity of SaOS-2 cells seeded on the silicon nitride scaffolds was quantified with osteogenic medium contained 1 μ L/mL L-ascorbic acid, 10 μ L/mL β -glycerophosphate on days 3, 7 and 10. The absorbances were measured according to the manufacturer's protocols at 405 nm.

2.6.4. Total protein assay

The total protein content of the cells on the silicon nitride scaffolds was determined with a BCA protein assay on 3, 7 and 10 days. The scaffolds were incubated in cell lysis buffer for the extraction of the proteins then centrifuged at 4 °C for 20 min. The samples were treated with BCA solution at 37 °C for 30 min then cooled at room temperature. The amount of total protein was measured at 562 nm.

2.6.5. Fluorescence microscopy and scanning electron microscopy (SEM) analyses

Viability of SaOS-2 cells on the silicon nitride scaffolds was determined with a Live/Dead assay on days 3, 7 and 10. Briefly, cells were stained with calcein-AM (0.5 μ L/mL) for live cells and ethidium homodimer-1 (EthD-1, 2 μ L/mL) for dead cells. Cells were incubated at 37 °C for 20 min and thoroughly washed with PBS for three times. The

stained cells were observed by fluorescence microscope. SaOS-2 cells were cultured on silicon nitride scaffolds for 14 days and cell morphology and adhesion were analyzed with SEM and fluorescence microscopy. For fluorescence observation; cells on the scaffold surface were fixed with 3.7% paraformaldehyde (v/v) in PBS solution for 20 min at room temperature. Samples were washed with PBS solution and 0.1% Triton X-100 were used for permeabilization. SaOS-2 cells on the scaffold surface were stained with DAPI and Alexa flour 555 for cell nuclei and cytoskeleton respectively. After incubation stained cells were observed by fluorescence microscopy (Zeiss Observer Z1). Cell attachment and cell spreading on the scaffold surface were investigated by using Quanta FEG scanning electron microscopy (FEL, Thermo Fisher Scientific). Fixed cells on the scaffold were dehydrated in graded ethanol series (50%, 70%, 80%, 90% and 100%) then dried in the vacuum oven. Samples were coated with a thin layer of gold with a current of 15 mA under vacuum before SEM analysis. Dispersion and presence of Silicon (Si), Oxygen (O), Nitrogen (N), Carbon (C), Potassium (P), Calcium (Ca) elements on the scaffold surface were investigated by Energy-Dispersive X-ray spectroscopy (EDX) and mapping analyses.

3. Results

3.1. Physical characterization of specimens

Silicon nitride ceramic was sintered under partial sintering conditions by limiting temperature and amounts of sintering additives. Therefore, a porous structure was obtained. The bulk density was measured as 2.74 g/cm³ and open porosity was 10.54%. The fine, porous structure of the sample (Fig. 1a) consisted of both equiaxed and rod-like grains. The lower aspect ratio of the rod-like grains resulted from low sintering temperature. MIP was used to estimate the porosity and pore size distribution of the silicon nitride. Fig. 1b shows the pore size distribution and according to MIP curve, the median pore size was 0.77 μ m. The presence of a peak in the curve suggests the typical monomodal porous structure. The XRD pattern (Fig. 1c) of the sample shows that β -silicon nitride was formed as a major phase with the entity of β -silicon

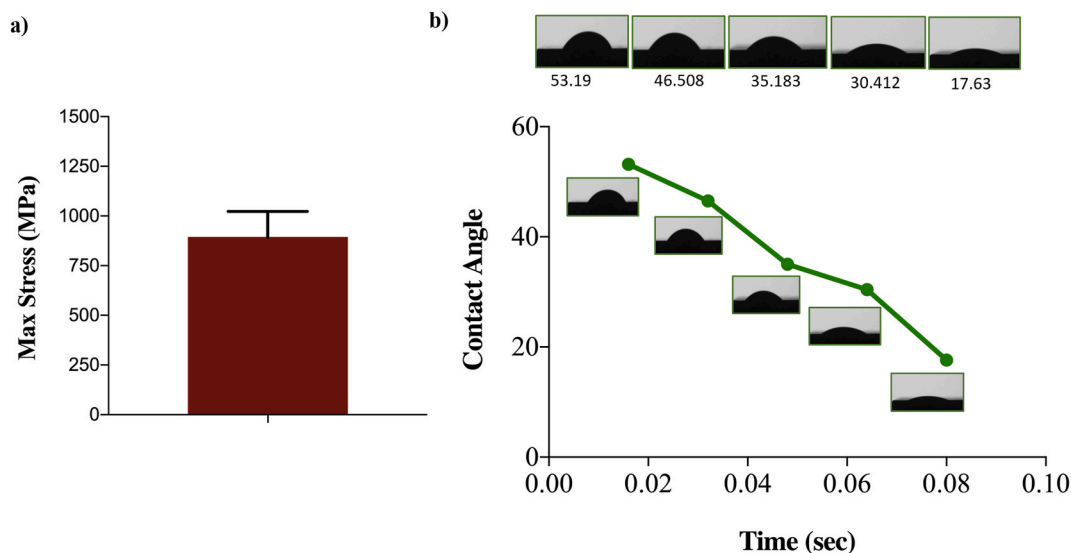


Fig. 2. a) Mechanical test result of the silicon nitride scaffold b) Static contact angle measurement of silicon nitride scaffold. (For interpretation of the references to color in this figure legend, the reader is referred to the Web version of this article.)

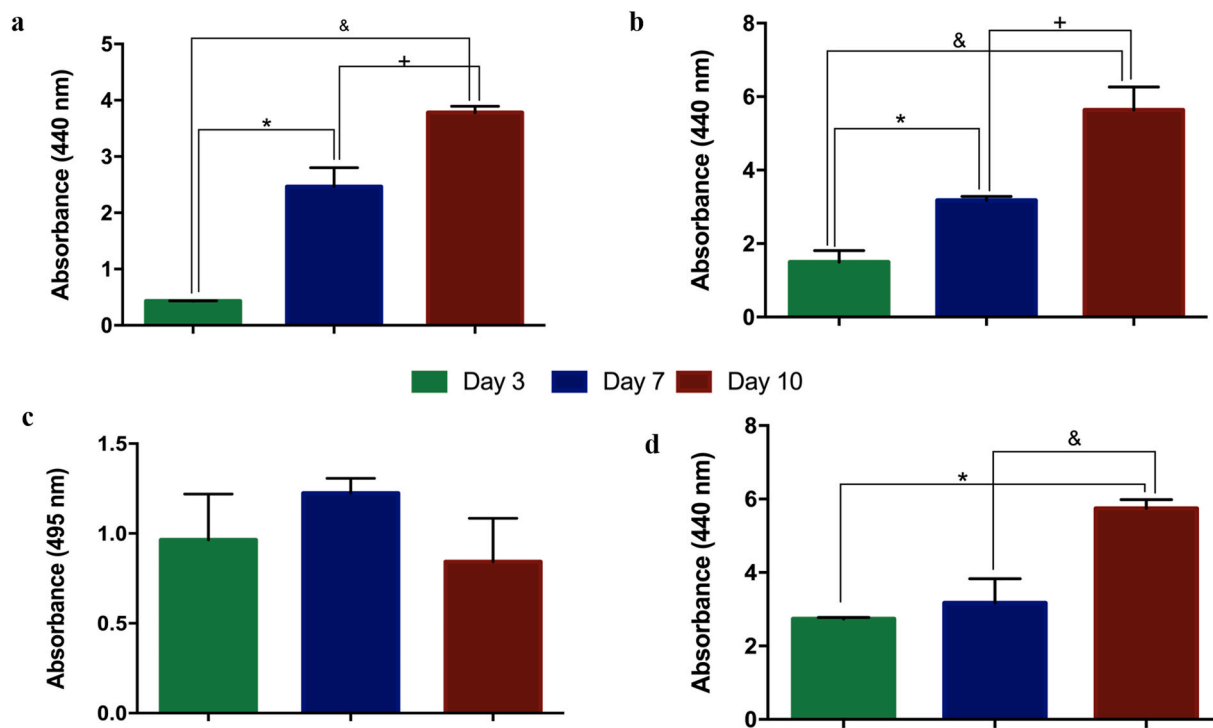


Fig. 3. *In vitro* study results of Saos-2 cells seeded on silicon nitride scaffold; a) ALP activity b) BCA assay c) Cytotoxicity with LDH assay d) Proliferation with WST-1 assay. (For interpretation of the references to color in this figure legend, the reader is referred to the Web version of this article.)

nitride. Not only sintering temperature but the lower amounts of sintering additives also retarded the transformation from α to β -silicon nitride by decreasing the amount of liquid phase formed during sintering where transformation occurred via solution and precipitation process.

3.2. Mechanical test of scaffolds

Mechanical properties of the silicon nitride scaffold were evaluated by the compression test. The compressive modulus of the scaffolds which calculated from the initial linear area of the stress-strain curves was found to be 893.16 MPa (Fig. 2a). A static contact angle analysis was performed to determine the wettability of the scaffolds. The contact

angle was measured from five different points of each sample and the average value was reported.

3.3. Contact angle measurement

Fig. 2b illustrates the behavior of the wettability of the surface. In contact angle measurement, when the water dropped on each point of the silicon nitride surface, the drop was immediately absorbed by the surface. The measured contact angle value was found as $36.646 \pm 5.2^\circ$. Silicon nitride surfaces showed highly hydrophilic properties. Thus, the surface of the membranes was considered to be suitable for protein and cell adhesion.

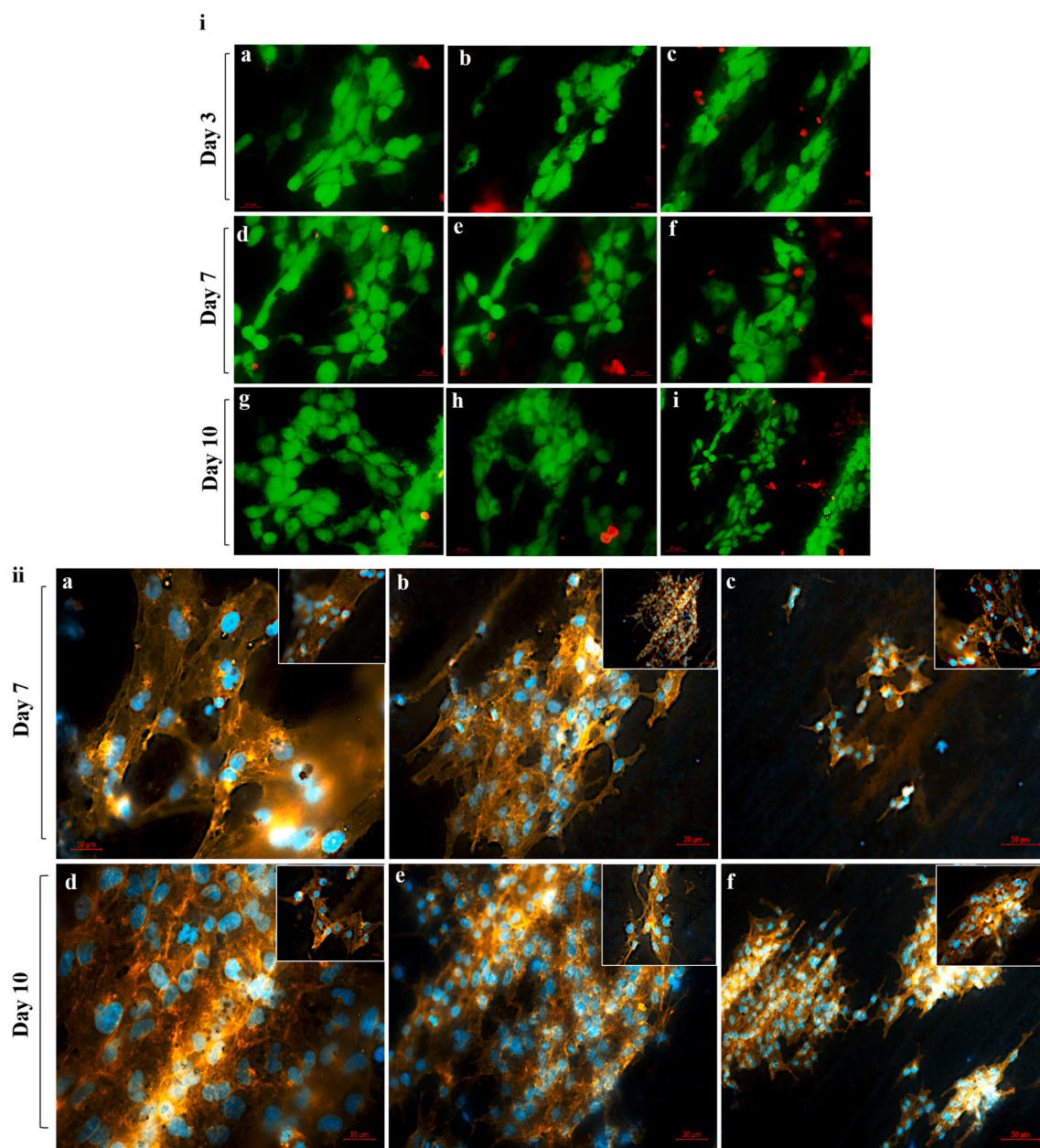


Fig. 4. i. Live/dead assay for SaOS-2 cells seeded on silicon nitride scaffolds after 3 (a,b,c), 7 (d,e,f) and 10 (g,h,i) days of culture ii. Actin/DAPI images of SaOS-2 cells for 7th and 10th day on silicon nitride scaffolds respectively. Cell attachment for 7th day (a,b,c); Cell attachment for 10th day (d,e,f). (For interpretation of the references to color in this figure legend, the reader is referred to the Web version of this article.)

3.4. *In vitro* studies

In vitro study results indicated that SaOS-2 cells proliferated gradually on silicon nitride for 10 days (Fig. 3). Cell proliferation increase rate was statistically significant at day 10, compared to the days 3 and 7. Cytotoxicity assay represented that silicon nitride did not show any cytotoxic effect on cells at all incubation times. ALP activity of the cells showed an increasing trend during the culture period. BCA assay was used to determine total protein content produced by cells. An increase in protein concentration was observed during the 10 days incubation period.

3.4.1. Fluorescence microscopy and scanning electron microscopy (SEM) analyses

Live-dead staining of SaOS-2 on silicon nitride (Fig. 4i) showed that cells adhered to silicon nitride and they were viable. On day 3, cells were

round and non-uniformly distributed. On days 7 and 10, cell population increased and cell shapes became lenticular with extensions. Cell spreading and attachment on the silicon nitride surface were determined by fluorescence microscopy for days 7 and 10. Cell nuclei and cytoplasmic extensions were observed in blue and orange color, respectively. As seen in Fig. 4ii, SaOS-2 cells were attached on silicon nitride scaffold surface with their cytoplasmic extensions on day 7. Also, cells proliferated and colonized on the surface of the scaffold on day 10. SEM images of a silicon nitride seeded with SaOS-2 cells for 7 and 10 days can be seen in Fig. 5(a–d). Cells were well attached and distributed on silicon nitride surface. On day 7, partial coverage of scaffolds with cells was observed (silicon nitride grains still can be seen) while at day 10, the surface was completely covered by SaOS-2 cells without an additional polishing procedure as a result of the smooth surface obtained by tape casting. Fig. 6 shows the EDX analysis indicating the distribution of Si, O, N, C, P, Ca in the silicon nitride surface. Silicon and nitrogen elements, which

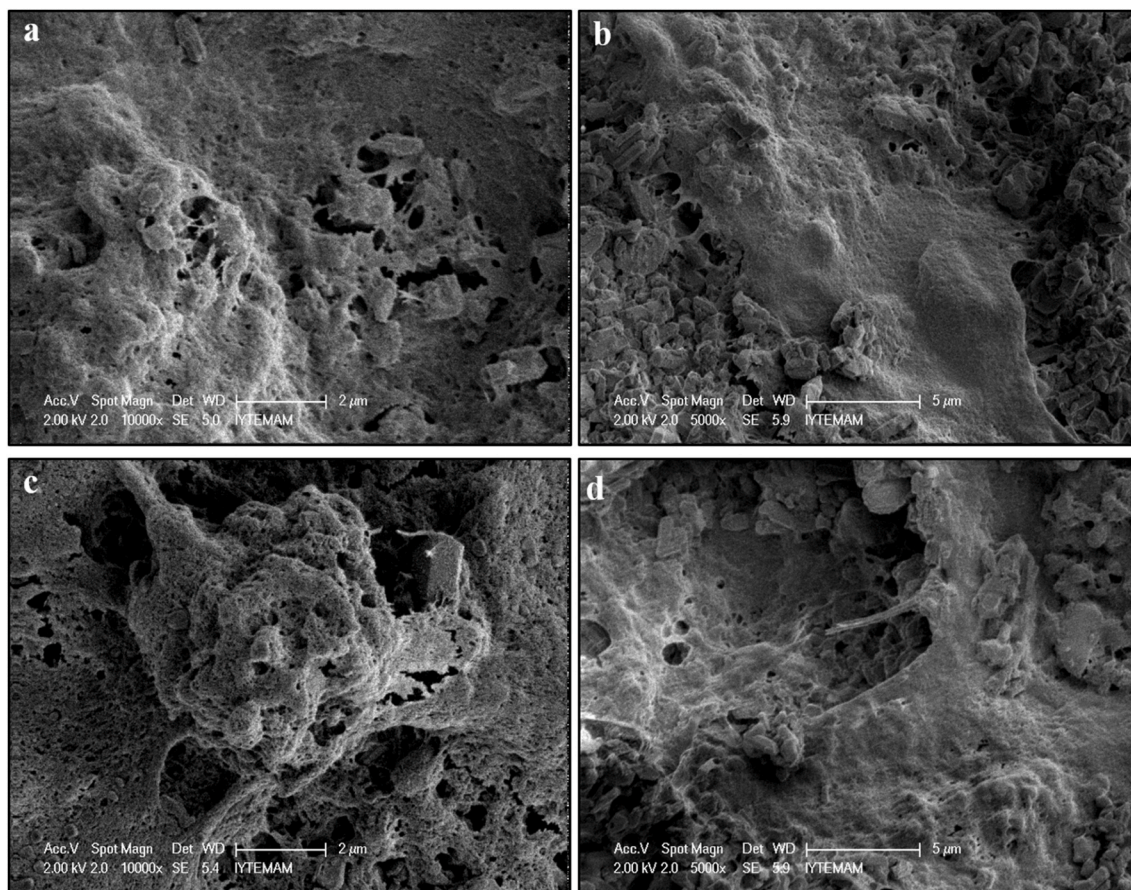


Fig. 5. SEM images of Saos-2 cells morphology evolutions on the silicon nitride of 7th day (a,b) and 10th day (c, d).

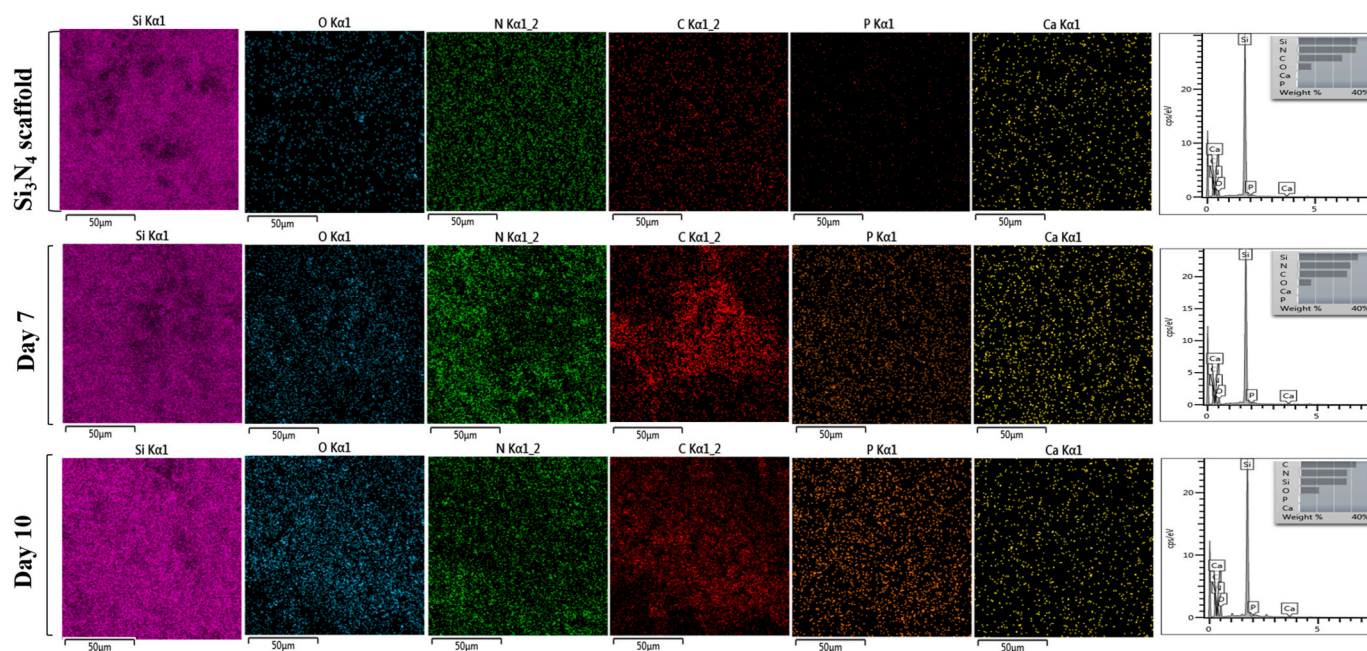


Fig. 6. EDX elemental and mapping analysis of Silicon (S), Oxygen (O), Nitrogen (N), Carbon (C), Phosphorus (P), Calcium (Ca) on Si₃N₄ scaffolds and after 7 and 10 days in cell culture. (For interpretation of the references to color in this figure legend, the reader is referred to the Web version of this article.)

are the main components of the scaffold, were detected on the surface, some amount of calcium that was used as sintering additives was also detected. As silicon nitride seeded with cells, the distribution of some

elements such as O, C, Ca, P were changed. The intensity of oxygen elements increased gradually for the samples seeded for 7 and 10 days. This proved attachment and further proliferation of SaOS-2 cells.

Furthermore, an increase in the intensity Ca elements was noticeable on the scanned area and P elements appeared after cell culture, confirming cell proliferation and mineral deposition by cells on the scaffold surface.

4. Discussion

In this study, we present engineering of porous silicon nitride ceramic fabricated by tape casting and partial sintering. We also examined the cytotoxicity and cell proliferation of the ceramic. The development of silicon nitride-based bioceramics produced either in dense or porous forms, depending on the application is an exciting approach in the field of biomaterials. There are several approaches in production of porous ceramics which are preferred because of their capacity to sustain the metabolic needs of the cells. For this reason, we applied partial sintering due to its advantages in comparison to other techniques. When a sacrificial template is used to form porosity, residue from the template can be introduced in ceramic that may have an adverse or toxic effect on the biological properties of ceramic. In another technique, replication, often a degradation in mechanical properties are obtained because of the defects generated in struts during the pyrolysis of the polymer template [20,21]. In partial sintering, the process is completed before densification and therefore, the porosity forms in the voids remaining between the necked grains [20,22,23]. Besides, we developed a standardized model system that can determine the functional effects of silicon nitride ceramic that was fabricated by tape casting and partial sintering. It should be noted that the fabrication of a silicon nitride ceramic was the key to the continuous adhesion and spreading of cells. Therefore, the surface of our material was carefully aligned during the assembling process and the material was further heated under nitrogen atmosphere at 1700 °C for 3 h for stabilization. SEM images of the sample (Fig. 1a) show a typical microstructure of partially sintered ceramic. Bonding of silicon nitride grains occurred before densification and uniform distribution of sub-micron pores can be observed. Cappi et al. compared two types of silicon nitride; sintered and hot-pressed and they reported that surface had an important influence, not on cell viability but cell proliferation [24–27]. Since sintered silicon nitride had surface porosity, it supported proliferation. Moreover, sub-micron porosity formed had a substantial contribution to cell growth. Evaluation of scaffolds in *in vitro* cell cultures showed that the silicon nitride scaffolds can retain their relatively stable architectures and mechanical properties during culture period (Fig. 2a). To enable sufficient cell spreading, microenvironments tunable towards compressive modulus and containing biologically active ceramic scaffolds are usually desired, which seldom satisfy the requirements for stress-strain properties due to their weak mechanical properties. In our study, SaOS-2 cells exhibited spreading on scaffold. In summary, cells mostly displayed normal spreading in the microenvironment. Observations on the cell morphology were in good agreement with the viability and proliferation data (Fig. 3). WST-1 assay results to quantify cell proliferation by measuring the metabolic activity indicated that silicon nitride ceramic to have no cytotoxicity on cells and promote cell proliferation in culture. With our approach, we improved the fabrication process and enhanced biocompatibility while holding the cytotoxicity in low levels in 3D cell culture. Morphological analyses were next performed. The viability levels of each day can easily be compared using the live-dead assay. Fluorescence images of cells show that cells tend to aggregate (Fig. 4) as small aggregates on scaffolds. Even on day 3, the extensions of SaOS-2 cells can be observed (Fig. 4i). The surface roughness is another important parameter for cell yield and proliferation in silicon nitride ceramics. Some of the *in vitro* studies emphasized the polishing of silicon nitride surface improved the cell yield and proliferative capacity. They reported that polishing provided a more suitable environment for bone cells hence higher cell yields and osteocalcin production were obtained [14,15]. Due to the smooth and defect-free surface produced by tape casting, successful cell adhesion and proliferation were observed without an additional polishing procedure. SaOS-2 cells were viable and

displayed more rounded morphology on day 3, however, for days 7 and 10 their shapes became more lenticular with the formation of extensions. F-actin/DAPI staining was further performed to monitor the spreading and morphology of cells. As expected, starting from day 7 through day 10, the cells gradually spread out to form initially spindle shapes, and later long stripe-like shapes due to the silicon nitride surface. The proliferation of cells was also prominent, eventually reaching confluence after 7 days of culture. The results provide a potential design map to choose desired fabrication methods in tissue engineering and regenerative medicine applications, which may be further expanded to predict the cell survival behaviors of various other ceramic types. One main limitation of the production of silicon nitride is its poor sinterability. Low diffusion coefficient of silicon nitride due to the higher amount of covalent bonding nature obstruct mass transport and densification. High sintering temperatures, external pressures, and addition of sintering additives should be used during the sintering of silicon nitride. However, this limitation has been benefited for the production of porous silicon nitride during this study by applying low sintering temperature and additives.

5. Conclusion

Biocompatibility and cell proliferation of porous silicon nitride produced by tape casting and partial sintering were investigated in the current study. Tape casting is enabled to obtain a smooth surface without any additional polishing procedures and having various dimensions such as thickness, width and length by lamination of the tapes. Silicon nitride surface produced maintained healthy cellular function. The silicon nitride ceramic fabricated by tape casting and partial sintering increased viability and cell survival. Finally, the use of this fabrication method provided biological signaling for cell growth to maintain 3D bone structure with possible candidates for substitution. The silicon nitride produced by tape casting and partial sintering is a potential candidate for use as bone grafts. This production method is easy and can be personalized for each patient who has different sizes and types of bone defects.

Declaration of competing interest

The authors declare that they have no known competing financial interests or personal relationships that could have appeared to influence the work reported in this paper.

Acknowledgements

The authors are grateful to Izmir Institute of Technology (IZTECH) Biotechnology and Bioengineering Research and Application Center (IZTECH BIOMER) for fluorescence microscopy analysis and Center for Materials Research (IZTECH CMR) for SEM and EDX analyses.

References

- [1] H. Wu, T. Liu, Z. Xu, J. Qian, X. Shen, Y. Li, Y. Pan, D. Wang, K. Zheng, A. R. Boccaccini, J. Wei, Enhanced bacteriostatic activity, osteogenesis and osseointegration of silicon nitride/polyetherketoneketone composites with femtosecond laser induced micro/nano structural surface, *Appl Mater Today* (2020), <https://doi.org/10.1016/j.apmt.2019.100523>.
- [2] F. Wang, J. Guo, K. Li, J. Sun, Y. Zeng, C. Ning, High strength polymer/silicon nitride composites for dental restorations, *Dent Mater.* 35 (2019) 1254–1263, <https://doi.org/10.1016/j.dental.2019.05.022>. Available from.
- [3] C. Goswami, I.K. Bhat, A. Patnaik, T. Singh, G. Fekete, Fabrication of ceramic hip implant composites: influence of silicon nitride on physical, mechanical and wear properties, *Silicon India* (2019), <https://doi.org/10.1007/s12633-019-00222-5>.
- [4] L. Zhang, X. Liu, M. Li, E. Xu, F. Zhao, H. Yuan, X. Sun, C. Zhang, L. Gao, J. Gao, Feasibility of SiAlON-Si₃N₄ composite ceramic as a potential bone repairing material, *Ceram. Int.* (2020), <https://doi.org/10.1016/j.ceramint.2019.09.150>.
- [5] F.A. Universität, E. Nürnberg, E. De, U.S. Ci, A. Kelnberger, R. De, 12, United States Patent 2 (2019).

- [6] A. Parsi, F. Golestani-Fard, S.M. Mirkazemi, The effect of gelcasting parameters on microstructural optimization of porous Si₃N₄ ceramics, *Ceram. Int.* (2019), <https://doi.org/10.1016/j.ceramint.2019.01.222>.
- [7] S. Fu, M. Zhu, Y. Zhu, Organosilicon polymer-derived ceramics: an overview, *J Adv Ceram* (2019), <https://doi.org/10.1007/s40145-019-0335-3>.
- [8] F. Yang, S. Zhao, Z. Yang, G. Chen, J. Chen, S. Yuan, Synthesis and characterization of outer shell strengthened Si₃N₄ foam ceramics, *Mater. Res. Express* (2019), <https://doi.org/10.1088/2053-1591/ab3597>.
- [9] H. Xie, L. Zhang, E. Xu, H. Yuan, F. Zhao, J. Gao, SIALON–Al₂O₃ ceramics as potential biomaterials, *Ceram. Int.* (2019), <https://doi.org/10.1016/j.ceramint.2019.05.221>.
- [10] E. Marin, T. Adachi, M. Zanocco, F. Boschetto, A. Rondinella, W. Zhu, S. Somekawa, R. Ashida, R.M. Bock, B.J. McEntire, B.S. Bal, O. Mazda, G. Pezzotti, Enhanced bioactivity of Si₃N₄ through trench-patterning and back-filling with Bioglass®, *Mater. Sci. Eng. C* (2020) <https://doi.org/10.1016/j.msec.2019.110278>.
- [11] Z. Badran, X. Struillou, F.J. Hughes, A. Soueidan, A. Hoornaert, M. Ide, Silicon nitride (Si₃N₄) implants: the future of dental implantology? *J. Oral Implantol.* (2017) <https://doi.org/10.1563/aid-joi-D-16-00146>.
- [12] M. Zanocco, E. Marin, A. Rondinella, F. Boschetto, S. Horiguchi, W. Zhu, B. J. McEntire, R.M. Bock, B.S. Bal, G. Pezzotti, The role of nitrogen off-stoichiometry in the osteogenic behavior of silicon nitride bioceramics, *Mater. Sci. Eng. C* (2019), <https://doi.org/10.1016/j.msec.2019.110053>.
- [13] Pezzotti, Marin, Zanocco, Boschetto, Zhu, McEntire, Bal, Adachi, Yamamoto, Mazda, Osteogenic enhancement of zirconia-toughened alumina with silicon nitride and Bioglass®, *Ceramics* (2019) <https://doi.org/10.3390/ceramics2040043>.
- [14] K.R. Awad, N. Ahuja, A. Shah, H. Tran, P.B. Aswath, M. Brotto, V. Varanasi, Silicon nitride enhances osteoprogenitor cell growth and differentiation via increased surface energy and formation of amide and nanocrystalline HA for craniofacial reconstruction, *Med DEVICES SENSORS* (2019), <https://doi.org/10.1002/mds3.10032>.
- [15] Y. Dai, L. Chu, Z. Luo, T. Tang, H. Wu, F. Wang, S. Mei, J. Wei, X. Wang, X. Shang, Effects of a coating of nano silicon nitride on porous polyetheretherketone on behaviors of MC3T3-E1 cells in vitro and vascularization and osteogenesis in vivo, *ACS Biomater. Sci. Eng.* (2019), <https://doi.org/10.1021/acsbomaterials.9b00605>.
- [16] M. Zanocco, F. Boschetto, W. Zhu, E. Marin, B.J. McEntire, B.S. Bal, T. Adachi, T. Yamamoto, N. Kanamura, E. Ohgitani, K. Yamamoto, O. Mazda, G. Pezzotti, 3D-additive deposition of an antibacterial and osteogenic silicon nitride coating on orthopaedic titanium substrate, *J. Mech. Behav. Biomed. Mater.* 103 (2020) 103557, <https://doi.org/10.1016/j.jmbbm.2019.103557>.
- [17] M.R. Loghman-Estarki, E. Mohammad Sharifi, H. Sheikh, A. Alhaji, M. Naderi, Development of biocompatibility in the orthodontic brackets based on MgAl₂O₄/Si₃N₄ nanocomposites, *Compos. B Eng.* (2019), <https://doi.org/10.1016/j.compositesb.2019.106989>.
- [18] H. Xin, H. Shi, W. Chen, J. Jia, W. Yang, Z. Jin, Tribological investigation of Si₃N₄-hBN on HXLPE bearing couple: effects of sliding velocity and contact load, *Ceram. Int.* (2019), <https://doi.org/10.1016/j.ceramint.2018.12.112>.
- [19] M. Eddaoudi, Characterization of Porous Solids and Powders: Surface Area, Pore Size and Density By S. Lowell (Quantachrome Instruments, Boynton Beach), J. E. Shields (C. W. Post Campus of Long Island University), M. A. Thomas, and M. Thommes (Quantachrome Instrument), *J. Am. Chem. Soc.* 127 (2005) 14117, <https://doi.org/10.1021/ja041016i>.
- [20] A. Choudhary, S.K. Pratihari, S.K. Behera, Single step processing of polymer derived macroporous SiOC ceramics with dense struts, *Ceram. Int.* (2019), <https://doi.org/10.1016/j.ceramint.2019.01.102>.
- [21] P. Sitthi-Amorn, J.E. Ramos, Y. Wang, J. Kwan, J. Lan, W. Wang, Matusik W. MultiFab, A machine vision assisted platform for multi-material 3D printing, *ACM Trans. Graph.* (2015), <https://doi.org/10.1145/2766962>.
- [22] R. Malik, Y.-W. Kim, I.-H. Song, High interfacial thermal resistance induced low thermal conductivity in porous SiC-SiO₂ composites with hierarchical porosity, *J. Eur. Ceram. Soc.* 40 (2020) 594–602, <https://doi.org/10.1016/j.jeurceramsoc.2019.10.056>.
- [23] M. Zhang, X. Li, M. Zhang, Z. Xiu, J.G. Li, J. Li, M. Xie, J. Chen, X. Sun, High-strength macro-porous alumina ceramics with regularly arranged pores produced by gel-casting and sacrificial template methods, *J. Mater. Sci.* (2019), <https://doi.org/10.1007/s10853-019-03576-8>.
- [24] A. Ali, B.N. Singh, S.K. Hira, S.P. Singh, R. Pyare, ZnO modified 1393 bioactive scaffolds with enhanced cytocompatibility and mechanical performance, *Ceram. Int.* (2020), <https://doi.org/10.1016/j.ceramint.2019.11.159>.
- [25] Z. Chen, Y. Xie, K. Li, L. Huang, X. Zheng, Synthesis of carbon coated-ceria with improved cytocompatibility, *Ceram. Int.* (2019), <https://doi.org/10.1016/j.ceramint.2019.06.256>.
- [26] N. Edwin, S. Saranya, P. Wilson, Strontium incorporated hydroxyapatite/hydrothermally reduced graphene oxide nanocomposite as a cytocompatible material, *Ceram. Int.* (2019), <https://doi.org/10.1016/j.ceramint.2018.12.002>.
- [27] B. Cappi, E. Özkol, J. Ebert, R. Telle, Direct inkjet printing of Si₃N₄: characterization of ink, green bodies and microstructure, *J. Eur. Ceram. Soc.* (2008), <https://doi.org/10.1016/j.jeurceramsoc.2008.03.004>.